

## Fast Electron Deposition in Laser Shock Compressed Plastic Targets

T. A. Hall,<sup>1</sup> S. Ellwi,<sup>1</sup> D. Batani,<sup>2</sup> A. Bernardinello,<sup>2</sup> V. Masella,<sup>2</sup> M. Koenig,<sup>3</sup> A. Benuzzi,<sup>3</sup> J. Krishnan,<sup>3</sup> F. Pisani,<sup>3</sup> A. Djaoui,<sup>4</sup> P. Norreys,<sup>4</sup> D. Neely,<sup>4</sup> S. Rose,<sup>4</sup> M. H. Key,<sup>4,\*</sup> and P. Fews<sup>5</sup>

<sup>1</sup>*Department of Physics, University of Essex, Colchester, United Kingdom*

<sup>2</sup>*Dipartimento di Fisica, Università degli Studi di Milano and INFN, Milan, Italy*

<sup>3</sup>*LULI, Ecole Polytechnique, Palaiseau, France*

<sup>4</sup>*Rutherford Appleton Laboratory, Chilton, Didcot, United Kingdom*

<sup>5</sup>*Department of Physics, University of Bristol, Bristol, United Kingdom*

(Received 23 January 1998)

We present the first results of fast electron deposition in a laser shock compressed plasma. The interaction of a 3 ps, 15 J laser pulse with solid polyethylene targets is used to produce fast electrons on one side of foil targets and a 2 ns duration laser pulse is used to drive a shock wave into the target from the opposite side.  $K_\alpha$  emission from chlorine fluor buried layers is used to measure the electron transport. The hot electron range in the shock compressed plastic is found to be approximately twice as large as the range in the solid density plastic. [S0031-9007(98)06642-3]

PACS numbers: 52.35.Tc, 52.50.Lp, 62.50.+p

The fast ignitor scheme [1] gives a possible route to reducing the energy required to achieve breakeven and gain in laser driven inertial confinement fusion (ICF). This scheme requires that an intense, short ( $\sim 10^{19}$  W cm<sup>-2</sup>, 10 ps) laser pulse produces fast electrons which are then absorbed in a small region of dense compressed plasma in order to produce local heating and ignition [2,3]. Previous experiments have been conducted to measure the fast electron production and the deposition of their energy in solid density targets and reasonable agreement has been obtained with models [4–6].

We report here experiments using the VULCAN laser to extend these measurements to the study of fast electron production and deposition in shock compressed plasmas using  $K_\alpha$  emission spectroscopy. The use of  $K_\alpha$  emission from buried layer fluors (fluorescent material) is now an established technique and has been widely used in the study of fast electrons from femtosecond laser plasma interactions [4,7].

The experiment can be divided into three parts: (i) the study of shock wave dynamics and the determination of the parameters of the shock compressed material, (ii) the characterization of the fast electrons temperature, and (iii) the comparison of  $K_\alpha$  emission from shock compressed and solid density material.

Fast electrons were produced on the “rear side” of plastic foil targets by focusing the VULCAN chirped pulse amplification (CPA) beam to a focal spot of 100  $\mu$ m diameter using an  $f/10$  off axis parabola (OAP). The energies of the CPA beam used in these experiments was in the range 4 to 15 J and the pulse length was 3 ps. Maximum irradiances on target were approximately  $6 \times 10^{16}$  W cm<sup>-2</sup>. The CPA beam was incident at 30° on the target in order to maximize laser absorption following previous experiments [4]. The foil targets were compressed using two, 108 mm diameter frequency doubled long pulse beams (2 ns) of the VULCAN laser

with a total energy of up to 160 J focused onto a spot of diameter 200  $\mu$ m using random phase plates (RPP). The shock compression laser pulses were incident on the targets from the “front side,” i.e., from the opposite side from the CPA beam. The targets in these experiments consisted of a PVC plastic fluor layer of 13.5  $\mu$ m thickness, sandwiched between two thicknesses of polyethylene. The thickness of the polyethylene layer on the rear side of the target was varied from 10 to 150  $\mu$ m. The front side polyethylene overlayer was 26  $\mu$ m. This front side overlayer prevented any excitation of the plastic fluor layer by the long pulse beams and also prevented any fast electrons from the CPA interaction zone from traveling around the target and hitting the fluor layer from the front side. Such fast electron excitation was observed to take place if this overlayer was omitted.

The chlorine  $K_\alpha$  spectra were recorded on Kodak DEF film [8] using three pentaerythritol flat crystal spectrometers. Two spectrometers were placed on the front side, one at near normal incidence and the other at approximately 60° incidence and one spectrometer was placed on the rear side at about 30° incidence. These positions and angles were mainly determined by beam constraints. The layout of the experiment is shown in Fig. 1.

Initial experiments were carried out using the long pulse beams alone to time the breakout of the shock by imaging the rear side of the target onto the slit of a visible streak camera [9]. The breakout was timed for various thicknesses of target. Figure 2 summarizes the results showing the breakout times for various thicknesses of plastic target. We also used two different laser energies in order to assess the influence of intensity fluctuations on compression parameters. Using these values of shock breakout time, the shock velocity can be evaluated. With this knowledge of the shock velocity, equation of state tables can be used to estimate the temperature

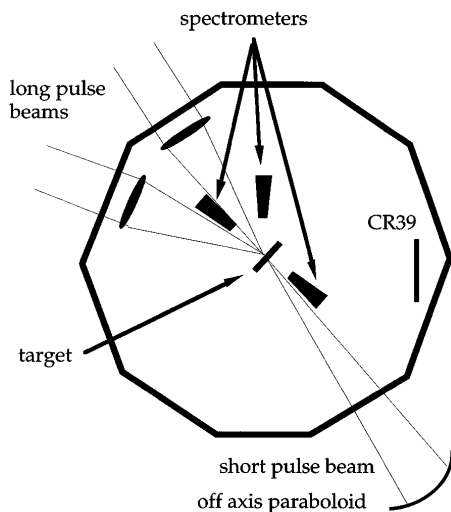


FIG. 1. Schematic diagram of the experimental setup. The CPA beam, turning mirror OAP and target are in the plane of the paper but the long pulse beams are incident out of the plane at approximately  $30^\circ$ .

and compression. SESAME EOS [10] tables predict a compression between 3 and 3.2 and temperatures in the range 7 to 8 eV. For the thickness targets, no optical emission at breakout was observed due to the weakening of the shock. This implies that the shock wave is slowing down towards the rear of the thicker targets. This slowing down can be seen in the experimental results shown in Fig. 2.

The 1D hydro code MULTI [11] was also used to model the results. The MULTI simulations are in good agreement with the simple estimates from the shock breakout time

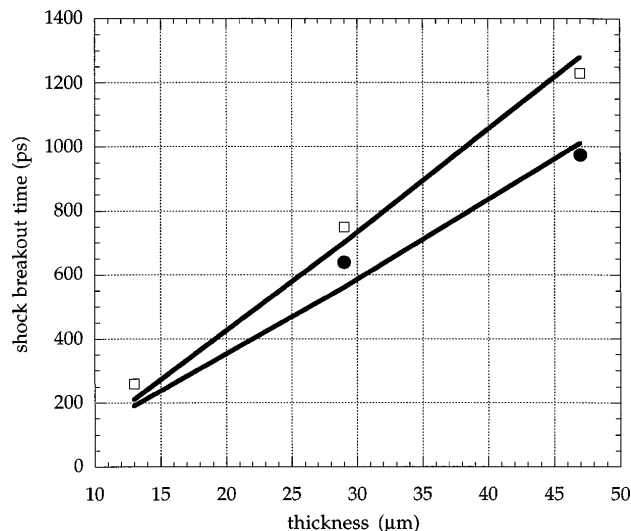


FIG. 2. Shock breakout time for three different thicknesses of plastic target. The open squares are the experimental values for an irradiance of  $1 \times 10^{14} \text{ W cm}^{-2}$  and the filled circles are for an irradiance of  $1.5 \times 10^{14} \text{ W cm}^{-2}$ . The continuous lines are the predictions from the MULTI code for the respective irradiances.

and show a uniformity of compression of  $\pm 15\%$  but also show that a rarefaction wave decompresses the front layers of the target. This rarefaction wave has not reached the fluor layer for any of the targets used at the time of the arrival of the CPA laser pulse. Two dimensional effects of the spreading of the shock front seem the most likely cause for the reduction of the shock velocity for the thicker targets. As we will see later the 2D effects have some consequences in the  $K_\alpha$  yield measurements.

Using the values of shock breakout time (measured for the thinner targets and extrapolated for the thicker targets), the short pulse beam was timed to be incident on the rear side  $\geq 100$  ps before shock breakout. This ensured that no expansion occurs from the rear side ahead of the arrival of the CPA pulse and all but a few microns of plastic is compressed (see later).

$K_\alpha$  spectra were obtained for a range of CPA laser pulse energies corresponding to irradiances up to  $6 \times 10^{16} \text{ W cm}^{-2}$  on target. This range of irradiance was chosen so as to match the expected fast electron range to the target thickness. The spectra were obtained for targets with and without shock compression.

On some laser shots, CR39 filtered track detector plastic [12] was used in the chamber in order to measure the proton energy spectrum and to get an indirect measurement of hot electron temperature [4].

The  $K_\alpha$  x-ray intensity was measured as a function of laser energy for one depth of buried fluor layer ( $10 \mu\text{m}$  plastic overlayer). The results show a quasilinear dependence on laser energy and as a result of this, for the remainder of this paper we use specific yields (yield per Joule incident laser energy). The use of specific yields is justified because the range of laser energies used is relatively small and any effect on the electron energy range is of secondary importance to the number of electrons produced. The specific  $K_\alpha$  yield is plotted in Fig. 3 as a function of depth of fluor layer for the solid density plastic. All points on the graph are averages over a number of laser shots and the value for each laser shot is the mean of the results from the three spectrometers. The error bar represents the standard deviation of these results.

The continuous curve is derived from the work of Harrach and Kidder [13] where the deposition  $\varepsilon(z)$  is of the form

$$\varepsilon(z) \propto \exp\left(-\beta\sqrt{\frac{z}{R_0}}\right)$$

with the value of  $\beta$  taken for carbon as 1.85. These values give the range  $R_0$  as  $3.7 \pm 1 \text{ mg cm}^{-2} \equiv 39 \pm 0.9 \mu\text{m}$ .

The hot electron temperature can be inferred from the model of Harrach and Kidder; we find

$$kT_{\text{hot}} = 20.6[R_0(kT_{\text{hot}})]^{0.56},$$

where  $kT_{\text{hot}}$  is in keV and  $R_0$  is in  $\text{mg cm}^{-2}$ . This gives a hot electron temperature of  $\sim 43$  keV. This value is

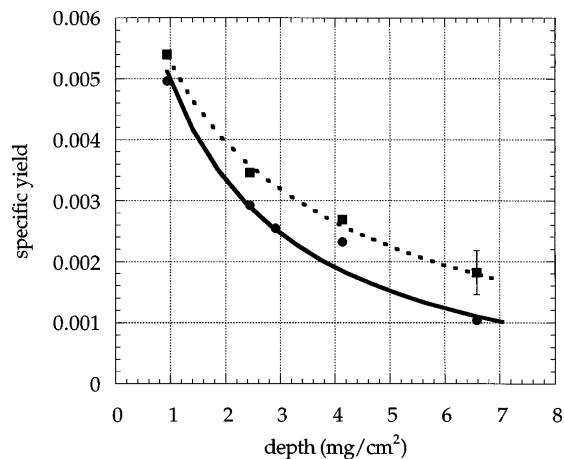


FIG. 3. Specific  $K_{\alpha}$  yields from solid density (●) and shock compressed (■) material as a function of depth of the buried fluor layer. The continuous line is due to the model of Harrach and Kidder for a curvilinear range of  $3.7 \text{ mg cm}^{-2}$  and the broken curve for a range of  $7.2 \text{ mg cm}^{-2}$ .

not too different from the value obtained from the CR39 measurements which gives the value of  $kT_{\text{hot}}$  in the range 25–50 keV dependent on laser irradiance. These values are also consistent with the hot electron temperature scaling given by Beg *et al.* [4]:

$$kT_{\text{hot}} \approx 100(I_{17})^{1/3} \text{ keV},$$

where  $I_{17}$  is the absorbed irradiance in units of  $10^{17} \text{ W cm}^{-2}$ . A hot electron temperature of 42 keV corresponds to an absorbed irradiance of  $7 \times 10^{15} \text{ W cm}^{-2}$ . The incident irradiances in these experiments were in the range  $10^{16} \text{ W cm}^{-2}$  to  $6 \times 10^{16} \text{ W cm}^{-2}$ .

The yields for the shock compressed plastic are also shown in Fig. 3. The values of yields for the shock compressed plastic lie above those for the solid density plastic in all cases. In these experiments, the areal density  $\rho z$  is constant. The broken line in Fig. 3 represents the yields in the shock compressed plastic fitted to the model of Harrach and Kidder. The range of the electrons in the shock compressed plastic is found to be  $7.2 \pm 2.0 \text{ mg cm}^{-2}$  compared to  $3.7 \pm 1.0 \text{ mg cm}^{-2}$  in the solid density plastic.

Not all the plastic between the fluor layer and the rear side is compressed. Careful measurements of the shock drive parameters, *a posteriori*, show that the thickness of the solid density plastic layer was on average  $\sim 8 \mu\text{m}$ . The *a posteriori* values of the thickness of the uncompressed material were obtained from the 1D simulations. The 2D effects that would slow down the shock for thicker targets will increase the thickness of this uncompressed layer above the values predicted by the 1D code. Thus the compressed range measurement for thicker targets contains a greater thickness of uncompressed material and the experimental values are likely to represent an underestimate of the change in the  $K_{\alpha}$  yield.

The yield results suggest that the number of electrons emerging from this  $8 \mu\text{m}$  boundary is identical in the two cases, within experimental error, and that the difference between the two sets of results is due to a difference in the ranges of the electrons. The difference in the ranges of the electrons may be due either to different energy spectra or as a result of different stopping powers.

The production of fast electrons could be affected by the shock compression if shock preheat were to cause some of the rear side material to spall or evaporate in advance of the CPA pulse arrival. Such an evaporation would provide a low density gas in front of the target prior to the arrival of the CPA pulse and thereby influence the absorption mechanism and hence fast electron production. Previous experiments [14,15] measuring the rear surface reflectivity and emissivity of shock compressed plastic targets under similar conditions have shown no preheat at these shock drive irradiances. This is confirmed by the form of the optical emission at shock breakout. Because of the similarity of the shock conditions in this experiment with those described in Ref. [14], we did not take any particular efforts to measure preheat in these experiments. A low density gas is produced by the laser pedestal due to finite contrast ratio of the CPA pulse [16] which is between  $10^{-6}$  and  $10^{-7}$  400 ps before the main pulse. This pedestal will create a plasma which would mask any long pulse shock preheat spall (if there were any).

Recent papers [17,18] have shown that the electrical conductivity plays a critical role in fast electron penetration. Bell *et al.* [18] describe the conditions when flux inhibition can restrict the penetration of fast electrons and change their energy spectrum. The penetration depth  $z_0$  given by Bell can be written in the form

$$z_0 = 3 \times 10^{-3} (kT_{\text{hot}})^2 \sigma_6 I_{17}^{-1} \mu\text{m},$$

where  $\sigma_6$  is the conductivity of the material in units of  $10^6 \Omega^{-1} \text{ m}^{-1}$ . The interaction of the CPA beam with the target rear side will create a hot, very dense plasma layer and the conductivity of the material inside the rear surface of the target is likely to change very dramatically in space and time and to be determined by the position of the heat front from the CPA pulse. Simulations using the hydro code MEDUSA [19] with multigroup nonlocal electron transport have been carried out to model the CPA pulse driven heat front. The results show that the position of the heat front 2 ps after the peak of the CPA pulse is  $2.5 \mu\text{m}$  from the original target surface with a shock wave preceding the heat front to a further  $1 \mu\text{m}$ . The temperature behind the heat front lies in the range 0.4 to 0.5 keV. Using these values of the electron temperature, we can estimate the electrical conductivity: From Spitzer, we find that  $\sigma_6 \approx 5$ . Using this value in Bell's formula for  $z_0$  we find that  $z_0 \approx 375 \mu\text{m}$ , i.e., much larger than the penetration depth of the heat front. At the heat front itself the temperature drops rapidly and the conductivity and  $z_0$  fall even more steeply to the values in the shock

front driven by the CPA pulse, so that, at the temperature in the shock region the value of  $z_0$  has fallen to  $\sim 0.4 \mu\text{m}$ . Thus, according to Bell's model, flux inhibition will be important in the surface layers determined by the plasma layer produced by the CPA pulse but cannot explain the differences observed in our experiments. Also, due to the rather low CPA laser intensity we used, magnetic fields effects will also not play any significant role [20].

The further possibility for the reason for the difference is due to dense plasmas effects on the stopping power of fast electrons. In particular in the case of compressed materials this is given by

$$\frac{dE}{dz} = -\frac{2\pi e^4}{E} (n_f L_f + n_b L_b),$$

where  $E$  is the electron energy,  $n_f$  and  $n_b$  are the densities of free and bound electrons, respectively, and  $L_f$  and  $L_b$  are the respective stopping numbers. In the cold material, there is only the contribution from bound electrons, plastic being an insulator. The effect on range can thus be explained by a reduction of the stopping number of bound electrons due to the increase in their effective ionization/excitation potential as a consequence of ionization. This can be described with the work of More [21] using the value of ionization ( $\approx 1.7$ ) obtained from the SESAME tables. The effect has been described in theoretical papers such as [2,22] considering both the cases of fast electrons and fast ions moving in a dense plasma. However, care should be taken in extrapolating these results to our case which is characterized by a lower temperature and hence higher degrees of degeneracy and correlation. A calculation of stopping power performed for the case of plastic, following Val'chuk *et al.* [23] yields a 30% reduction of the stopping power in the compressed material consistent with our results.

In conclusion, we have presented the first results for fast electron deposition energy in shock compressed matter. The irradiances used in these experiments are lower than would be used in the fast ignitor scheme but the significance of the results is, nevertheless, very relevant to this scheme. It is shown that in the experiments presented here that ionized, compressed plastic is less effective at stopping the fast electrons than solid density, un-ionized plastic. The stopping power of the compressed material is reduced (in areal density units) over the solid density materials.

These experiments are the first measurements of electron stopping power in compressed plasmas and are relevant to transport studies in dense laser produced plasmas,

but further experiments with more highly compressed plasmas are necessary before the results may be safely extrapolated to fast ignitor conditions.

This work has been supported by the E.U. Programme: TMR Laser Facility Access (Contract No. ERBFMGEC950053) and by the LEA "High Power Laser Science." The participation of V.M. has been possible also thanks to an ERASMUS grant obtained in the framework of the PIC coordinated by Professor L. Lanz of the University of Milan. We also thank the staff at the Central Laser Facility, Rutherford Appleton Laboratory for their very considerable help before and during the experiment.

---

\*Present address: LLNL, Livermore, CA 94551.

- [1] M. Tabak *et al.*, Phys. Plasmas **1**, 1626–1634 (1994).
- [2] C. Deutch, H. Furukawa, K. Mima, M. Murakami, and K. Nishihara, Phys. Rev. Lett. **77**, 2483–2486 (1996).
- [3] S. Atzeni, Jpn. J. Appl. Phys. **34**, 1980 (1995).
- [4] F.N. Beg *et al.*, Phys. Plasmas **4**, 447–457 (1997).
- [5] G. Malka and J.L. Miquel, Phys. Rev. Lett. **77**, 75–78 (1996).
- [6] S.C. Wilks, W.L. Kruer, M. Tabak, and A.B. Langdon, Phys. Rev. Lett. **69**, 1383–1386 (1992).
- [7] R.C. Mancini *et al.*, J. Phys. B **27**, 1671 (1994).
- [8] P.D. Rockett *et al.*, Appl. Opt. **24**, 2536–2542 (1985).
- [9] M. Koenig *et al.*, Phys. Rev. E **50**, R3314 (1994).
- [10] "SESAME, The LANL equation of state database," LANL Report No. LA-UR-923407, 1992.
- [11] R. Ramis, R. Schmalz, and J. Meyer-ter-Vehn, Comput. Phys. Commun. **49**, 475 (1988).
- [12] A.P. Fews *et al.*, Phys. Rev. Lett. **73**, 1801–1804 (1994).
- [13] R.J. Harrach and R.E. Kidder, Phys. Rev. A **23**, 887–896 (1981).
- [14] A. Benuzzi *et al.*, Phys. Plasmas **5**, 6 (1998).
- [15] A. Benuzzi *et al.*, Phys. Rev. E **54**, 2162 (1996).
- [16] C.N. Danson *et al.*, Opt. Commun. **103**, 392–397 (1993).
- [17] M.E. Glinsky, Phys. Plasmas **2**, 2796–2806 (1995).
- [18] A.R. Bell, J.R. Davis, S. Guerin, and H. Ruhl, Plasma Phys. Controlled Fusion **39**, 653–659 (1997).
- [19] A. Djaoui and A. Offenberger, Phys. Rev. E **50**, 4961 (1994).
- [20] J.R. Davis, A.R. Bell, M.G. Haines, and S.M. Guérin, Phys. Rev. E (to be published).
- [21] R.M. More, in *Fundamental Forces: Proceedings of the 27th Scottish Universities Summer School in Physics*, St. Andrews, 1984 (Scottish Universities Summer Schools, Edinburgh, 1985), pp. 157–214.
- [22] M.M. Basko, Sov. J. Plasma Phys. **10**, 689–694 (1984).
- [23] V.V. Val'chuk, N.B. Volkov, and A.P. Yalovets, Plasma Phys. Rep. **21**, 159–164 (1995).